tributed to a mixture of $TCNQ^0$ and low-lying $TCNQ^-$ states.

Finally, in Table I we summarize the level assignments in TTF-TCNQ made from the present work and draw a comparison with Ref. 1. We note that several uncertainties in the earlier assignments are clarified by our results, and that semiquantitative experimental evidence now exists for overlapping TTF^+ and $TCNQ^-$ states near E_F. Also indicated in Table I are those symmetry labels of the assigned states which can be determined from available calculations for the neutrals and the ions.

We wish to thank G. Castro, U. T. Muller-Westerhoff, and R. Schumaker for providing sample materials, P. McKernan, S. Werner, and F. Peters of the Stanford Tube Laboratory for their help with equipment, and J. A. Hertz for helpful discussions.

*Work at Stanford supported by the National Science Foundation through the Center for Materials Research at Stanford University.

[1]W. D. Grobman, R. A. Pollak, D. E. Eastman, E. T. Maas, Jr., and B. A. Scott, Phys. Rev. Lett. 32, 534 (1974).

[2]P. Nielsen, A. J. Epstein, and D. J. Sandman, Solid State Commun. 15, 53 (1974).

[3]C. J. Fritchie and P. Arthur, Acta. Crystallogr. 21, 139 (1966).

[4]J. P. Ferraris, D. O. Cowan, V. Walatka, and J. H. Perlstein, J. Amer. Chem. Soc. 95, 948 (1973); L. B Coleman, M. J. Cohen, D. J. Sandman, F. G. Yamagishi, A. F. Garito, and A. J. Heeger, Solid State Commun. 12, 1125 (1973).

[5]R. S. Bauer, Ph. D. dissertation, Stanford University, 1970 (unpublished).

[6]There are two stoichiometries of Cs-TCNQ. The most favorable one is $Cs_2(TCNQ)_3$. Associated with every two Cs in this compound there are one $TCNQ^0$ and two $TCNQ^-$ molecules distinguishable in x-ray diffraction. E. T. Maas, Jr., Mater. Res. Bull. 11, 873 (1974), established that exposure of Cs solid to TCNQ vapor forms bulk $Cs_2(TCNQ)_3$. In our case we expose TCNQ solid to Cs vapor. Although there is some uncertainty, we feel that it is much more likely that we have obtained $Cs_2(TCNQ)_3$ than Cs(TCNQ).

[7]A. J. Berlinsky, J. F. Carolan, and L. Weiler, Solid State Commun. 15, 795 (1974), and to be published.

[8]I. P. Batra, B. I. Bennett, and F. Herman, to be published.

[9]R. P. Shibaeva and L. O. Atovmyan, J. Struct. Chem. (U.S.S.R.) 13, 514 (1972).

[10]Since the UPS experiment involves an optical excitation event on a time scale of about 10^{-15} sec, the observed charge localization can be rigorously said to take place on time scales of this magnitude or smaller, as has been discussed elsewhere (Ref. 2). Hopping or other charge motion may take place more slowly; however, x-ray results for $Cs_2(TCNQ)_3$ indicate localization in that material for much longer times.

[11]Maas, Ref. 6.

[12]H. Johansen, to be published.

[13]T. E. Phillips, T. J. Kistenmacher, J. P. Ferraris, and D. W. Cowan, J. Chem. Soc., Chem. Commun. 14, 471 (1973).

Angular-Resolved Secondary-Electron–Emission Spectra from Tungsten Surfaces

Roy F. Willis

Surface Physics Group, Astronomy Division, European Space Research Organisation, Noordwijk, Holland

(Received 29 October 1974)

Energy-distribution spectra have been measured for secondary electrons backscattered into a narrow angle about the normal direction to three tungsten-single-crystal faces, viz. (100), (110), and (111). Improved spectral resolution provides evidence for emission from excited states located above the vacuum level, the intensity of emission being related to one-dimensional density-of-states features along the corresponding low-index symmetry lines. Good agreement with a calculated energy-band structure is observed.

Inelastic electron-electron scattering, which occurs during the screened Coulombic interaction between incident "primary" electrons and the valence electrons in a solid, produces fine structure in the energy-distribution curve (EDC) of emitted "secondary" electrons. First-order time-dependent perturbation theory[1] of electron-hole pair production and relaxation processes predicts an EDC which contains one-electron density-of-final-states features superimposed on a smoothly varying curve (the "cascade background" of inelastic multiply scattered electrons). Secondary-electron-emission (SEE) spectroscopy thus provides detailed information on the density

of *unfilled* states located above the vacuum level E_v of solids.

To date, however, SEE spectra, showing well-resolved final-states structure,[2] have generally been obtained with analyzers which collect over large emission angles [typically 100° to 180° collection angle with commercial low-energy-electron-diffraction (LEED)–Auger type display systems]. This is equivalent to integrating scattering out of final states in $\vec{K}$ space over a large *volume* of the Brillouin zone,[3] leading to an overall "smeared-out" distribution containing a limited amount of spectral detail. One way of improving matters is to limit the extent of $\vec{K}$ space sampled by recording spectra for emission into a small-angle selective analyzer. Recent photoemission measurements[4] of electrons restricted to a relatively narrow angle ($\lesssim 12°$) of emission about the directions normal to low-index tungsten single-crystal surfaces have shown that the EDC's reflect features relating to photoexcitation and emission from electron states which have their wave vectors confined to those symmetry lines that correspond to the crystal-surface normals. The geometry is such that the component of the excited- or final-state wave vector parallel to the surface is small, $\vec{K}_{\parallel} \to 0$, and remains unchanged during transmission through the surface. Energy-dependent refraction effects are therefore negligible.

In this paper, we have extended the above measurements[4] to the case of secondary-electron emission normal to the principal low-index faces (100), (110), and (111) of tungsten. The object was not only to improve spectral resolution, but to observe effects due exclusively to scattering from excited Bloch states in crystals free from any "mixing" due to transition matrix elements involving *initial* filled states, as occurs in photoemission.[5] An advantage of the angular-resolved technique is that, since the spectral fine structure relates essentially to a one-dimensional density of states located along a principal symmetry *line*, general points throughout the Brillouin zone being excluded, the method greatly facilitates the interpretation of final-states features in terms of existing energy-band calculations. The results confirm this. Greatly improved SEE spectral resolution was obtained, and the fact that good agreement with a calculated energy-band structure is observed for all three faces provided a self-consistent check on the interpretation of SEE spectra in terms of density-of-final-states structure. In addition, the work verifies that final-state crystal-momentum information is preserved to a large degree in the transport and escape steps of SEE.[6]

The experimental arrangement is shown schematically in Fig. 1. The SEE spectra were measured with a 130°-sector electrostatic analyzer with an energy resolution of 0.5% equivalent to an angular resolution of the order of less than 0.1°, as defined by the entrance slit of the analyzer. Tungsten single crystals were cut to expose the low-index planes to an accuracy within 3° and, after a standard cleaning procedure, were oriented within 1°.[7] The sample surfaces were regularly checked *in situ* for cleanliness and structure by a LEED-Auger display system, the first grid of which was grounded in order to provide a drift region free from electrostatic fields.[7] Ambient magnetic fields were reduced below 10 mG by enclosing the scattering and analyzing region completely with Mumetal shells. The electron beam was incident at an arbitrary angle of 45° to the crystal-surface normal and had a beam-energy spread of the order of 0.3 eV.

Energy-distribution spectra of secondary electrons emitted normal to tungsten (100), (110), and (111) faces are shown in Figs. 2(a)–2(c), respectively. The calculated density of states $D(E)$ and the energy bands along the corresponding ⟨100⟩ (ΓH), ⟨110⟩ (ΓN), and ⟨111⟩ (ΓP) symmetry lines are shown superimposed for comparison with the experimental spectra. The calculated energy-band structure[8] is limited to energies $E_k \lesssim 20$ eV in the case of the (100) face and $E_k \lesssim 13$ eV for the (110) and (111) orientations. We will concentrate, therefore, on those features in the SEE spectra which are covered by these energy ranges.[9] Peaks in the $D(E)$ curve assume a *constant* Lorentzian full-half-width broadening of 0.3 eV and show good agreement with peaks in the SEE spectra for energies $E_k \lesssim 10$ eV. Lifetime broadening of the excited states[10] *increases* with increasing

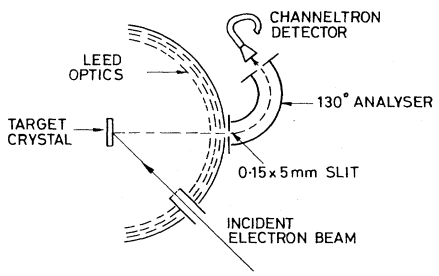

FIG. 1. Schematic diagram of the experimental apparatus.

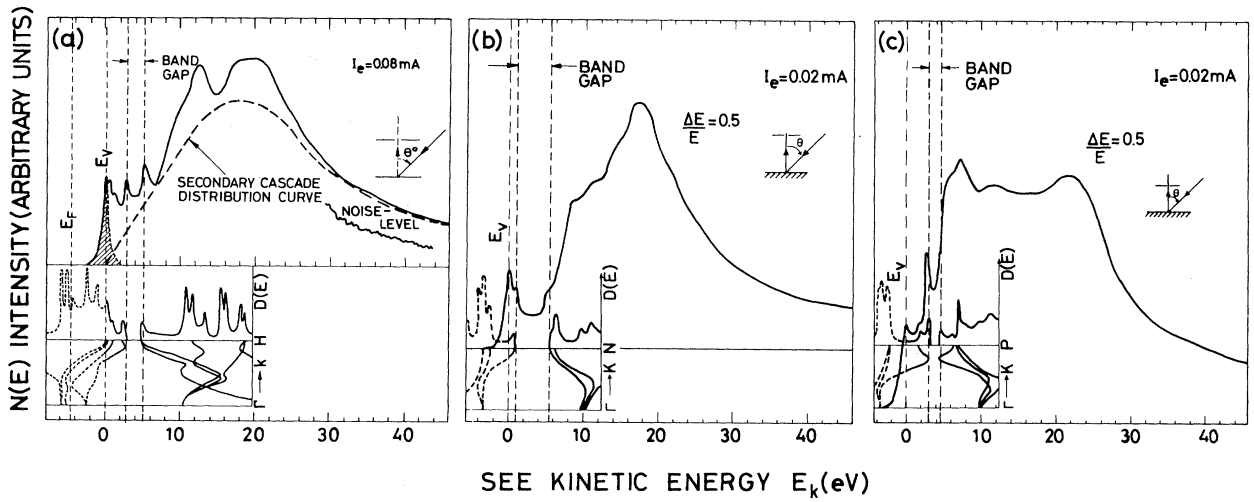

FIG. 2. Energy-distribution spectra, $N(E)$ versus E_k, of secondary electrons emitted normal, $P_{\parallel} \approx 0$, to (a) W(100), (b) W(110), and (c) W(111) faces for primary beam energy $E_p = 107$ eV. A small negative potential, $V_s = -0.75$ V, was applied to the target crystal. The intensity with reference to other spectra, obtained under otherwise identical conditions, is defined in terms of arbitrary parameters I_e (mA), the electron-gun filament emission current, and a scaling or magnification parameter of 4. The calculated density of final states, $D(E)$ versus E, and the energy-band structure along the ⟨100⟩ (a), ⟨110⟩ (b), and ⟨111⟩ (c) symmetry lines are shown for comparison, together with the relative positions of the Fermi level E_F and the vacuum level E_v. The SEE kinetic energy E_k (eV) is referred to E_v. The SEE cascade distribution curve together with the cross-hatched peak at $E_k = 0$ eV has not been emphasized for clarity in (b) and (c).

energy E_k, as can be seen by the increasing full width at half-height (FWHH) of peaks in the SEE spectral fine structure. Another possibility is that arising from "momentum" broadening of the final-state Bloch wave at the surface, which increases as the inelastic scattering length $L(E)$ decreases with increasing energy.[11] Both mechanisms lead to a smearing out of the calculated $D(E)$ fine structure for energies $E_k \gtrsim 10$ eV. However, the envelope of the calculated $D(E)$ fine structure continues to show good agreement with the broad features superimposed on the "secondary-cascade distribution curve" [shown schematically in Fig. 2(a)] at these high energies.[9] The shaded peak at $E_k = 0$ eV [Fig. 2(a)] appears in all three SEE spectra and is spurious in that it is due to scattering effects in the LEED-optics grids at the entrance to the analyzer (Fig. 1).

A real test of the degree of correlation between the experimental and theoretical results is provided by the fact that the calculated band structure exhibits gaps in the final states of varying width and energetic position along the three principal symmetry directions, Δ ⟨100⟩, Σ ⟨110⟩, and Λ ⟨111⟩. These gaps are clearly resolved as minima in the SEE spectra, extending from $2.5 < E_k < 4.5$ eV for the (100) face [Fig. 2(a)], $0.8 < E_k < 5.4$ eV for the (110) face [Fig. 2(b)], and $3.2 < E_k < 4.4$ eV for the (111) face [Fig. 2(c)], in good agreement with the calculated $D(E)$.[8] The significance of this result is that these band gaps occur only about the symmetry lines associated with emission normal to the respective crystal faces; the integrated density-of-final-states curve for the full Brillouin zone shows no gaps. Also, gaps in the final-states energy-band structure of tungsten were not predicted at these energies by previous calculations.[12] The SEE spectra, Fig. 2, not only endorse Christensen and Feuerbacher's recent calculations,[8] but also provide a critical test of their accuracy for energies far above the Fermi level E_F.

Another point to emerge is that the resolution of clearly defined band gaps about specific symmetry directions indicates that umklapp scattering contributions from other directions in the Brillouin zone do not superimpose significant additional structure.

Angular anisotropies in SEE arise from the conditions imposed at the surface by conservation of parallel momentum and selective wave matching between the emitted electronic plane wave, $\exp i(\vec{p}\cdot\vec{r})$, and the various Fourier components of the excited-state Bloch function,[13] which is characterized as a linear combination of plane waves:

$$\psi_K(\vec{r}) = \exp(i\vec{K}\cdot\vec{r}) \sum_G u_{K,G} \exp(i\vec{G}\cdot\vec{r}); \qquad (1)$$

i.e., as in LEED intensity calculations,[14] the wave-matching condition requires selective matching not only with plane-wave components whose parallel wave vectors $\vec{K}_{\parallel} = \vec{P}_{\parallel}$, but also with various Fourier components $(\vec{K}_{\parallel} + \vec{G}_{\parallel})$, where $\vec{G}_{\parallel}$ is the component parallel to the surface of any reciprocal-lattice vector. Fourier components $\exp[i(\vec{K} + \vec{G}) \cdot \vec{r}]$ can be translated into reduced wave vectors $\vec{K}$ by subtracting the reciprocal-lattice vectors $\vec{G}$. The energy distribution of emitted secondary electrons $N(E)$ can be related to the energy distribution of excited electrons $S(E, K)$, isotropically distributed inside the solid, by an escape probability function $T(E, K)$[3]:

$$N(E) = \int T(E, K) S(E, K)\, dK. \quad (2)$$

In an anisotropic emission model, $T(E, K)$ may be written[6] as

$$T(E, K) = \hat{S}_{hkl} \cdot \vec{T}(E_n(\vec{K})), \quad (3)$$

where $\hat{S}_{hkl}$ is a unit vector normal to the (hkl) surface and $\vec{T}(E_n(\vec{k}))$ is the surface transmission probability of a final-state electron of energy $E_n(\vec{K})$, wave vector $\vec{K}_n$, and band index n; i.e., Eq. (3) yields only those emission features which correspond to a final-state wave function that describes those electrons which can escape through a particular (hkl)-oriented surface. The geometry used here, Fig. 1, further restricts emission from those excited states with wave vector $\vec{K}_n$ confined along a symmetry line corresponding to the low-index face under consideration. The observed SEE fine structure is produced by electrons in excited states throughout the whole reduced zone[3] which have undergone inelastic scattering, just prior to escape, into those final states which happen to be on the symmetry line corresponding to the crystal-surface normal. The condition $\vec{K}_{\parallel} \to 0$ is such that umklapp contributions, arising from electrons moving inside the solid in a non-normal direction that are diffracted to the normal direction, are degenerate with the final-state wave function along the symmetry-line normal.[15] Final-state momentum information is then preserved to a large degree during the final transport and escape process. Umklapp and other "multiple-scattering effects"[14] are expected to become more important, however, with increasing polar angle θ, away from a symmetry direction, causing the SEE energy distributions to vary in a complex way.[16]

The angular-resolved SEE spectra for emission normal to low-index crystal faces presented here appear to show features representative of emission from *bulk* final states. This suggests that bulklike scattering mechanisms apply even close to the surface, in view of the low penetration depth of primary electrons ($\lesssim 10$ Å) for beam energies, $E_p \approx 100$ eV, and the mean depth of escape of secondaries ($\lesssim 10$ Å) in metals.[17] However, until a more detailed analysis of the SEE spectral line-shape and angular measurements have been carried out, it is not possible to dismiss contributions due to purely "surface" effects.[8] Indeed, the present results suggest that by limiting the extent of emission from general regions of K space, angular-resolved SEE should provide a valuable technique for unambiguously identifying not only contributions from *bulk* final states, but also mechanisms involving scattering from excited *surface* states and resonances associated with both clean and adsorbate-covered surfaces.

I am grateful to M. R. Barnes for his expert technical assistance with the measurements and to Dr. N. Egede Christensen, Dr. B. Feuerbacher, and Dr. B. Fitton for their photoemission results and calculations (prior to publication), and valuable comments. I also thank Professor J. M. Blakely for kindly supplying the tungsten single crystals.

---

[1]E. O. Kane, Phys. Rev. 159, 624 (1967).

[2]Here we concern ourselves specifically with that fine structure which appears as discrete maxima and minima in SEE *energy-distribution* curves at kinetic energies $E_k \lesssim 30$ eV; R. F. Willis, B. Feuerbacher, and B. Fitton, Phys. Lett. 34A, 231 (1971), and Phys. Rev. B 4, 2441 (1971). Weaker structure resolved in *derivative* spectra associated with Auger relaxation, temperature-dependent diffraction processes [see E. G. McRae, Surface Sci. 44, 321 (1974)], etc., usually occurs at higher kinetic energies and is not to be confused with the features arising from density-of-final-states effects discussed in the present paper.

[3]R. F. Willis, B. Fitton, and G. S. Painter, Phys. Rev. B 9, 1926 (1974).

[4]B. Feuerbacher and B. Fitton, Phys. Rev. Lett. 30, 923 (1973).

[5]The importance of angular anisotropies in *photoemission* due to the Bloch character of the *final* states has recently been emphasized by A. Liebsch, Phys. Rev. Lett. 32, 1203 (1974). However, in photoemission, *initial*-states effects also give rise to angular anisotropy [J. W. Gadzuk, Solid State Commun. 15, 1011 (1974)], which mixes in with that arising from selective wave matching of the excited final-state Bloch function at the surface.

[6]W. D. Grobman and D. E. Eastman, Phys. Rev. Lett. 33, 1034 (1974), have recently reached the same con-

clusion from an analysis of photoemission data.

[7]The SEE spectra were insensitive to variations in polar angle θ, or azimuthal angle φ, up to 5° off normal direction at the crystal face. The spectra were, however, found to be extremely sensitive to strong electrostatic patch-field effects in the vacuum chamber, particularly those features appearing at $E_k \lesssim 10$ eV. These effects could be balanced by the careful adjustment of a small negative potential, $V_s \simeq -0.75$ V, on the target crystal.

[8]N. E. Christensen and B. Feuerbacher, Phys. Rev. B 10, 2349 (1974); N. E. Christensen, unpublished.

[9]Evidence to support a correlation between maxima in SEE spectra and density-of-final-states fine structure for energies $E_k \gtrsim 10$ eV has been published [see Refs. 2 and 3].

[10]E. O. Kane, J. Phys. Soc. Jpn., Suppl. 21, 37 (1966).

[11]E. A. Stern, Phys. Rev. 162, 565 (1967).

[12]L. F. Mattheiss, Phys. Rev. 139, A1893 (1965); I. Petroff and C. F. Viswanathan, Phys. Rev. B 4, 799 (1971).

[13]G. D. Mahan, Phys. Rev. B 2, 4334 (1970).

[14]J. B. Pendry, J. Phys. C: Proc. Phys. Soc., London 2, 2273 (1969).

[15]This is equivalent to stating that Fourier components $\exp[i(\vec{K}_{\parallel}+\vec{G}_{\parallel})\cdot\vec{r}] \equiv \exp i(\vec{K}_{\parallel}\cdot\vec{r})$ in the reduced-zone scheme, $\vec{K}_{\parallel} \to 0$, for emission along a surface-normal *symmetry* direction.

[16]Preliminary results on the variation of secondary-electron spectra with polar angle $0 < \theta < 70°$ have been presented; R. F. Willis, in Proceedings of the Fourth International Conference on Vacuum Ultraviolet Radiation Physics, Hamburg, Germany, July 22–26 1974 (to be published).

[17]C. J. Powell, Surface Sci. 44, 29 (1974).

Angle-Resolved Secondary-Electron–Emission Spectra from Si(111)7×7 Surface States*

P. E. Best
Department of Physics and Institute of Materials Science, University of Connecticut, Storrs, Connecticut 06268
(Received 11 November 1974)

In angle-resolved secondary-electron–emission spectra from a silicon (111)7×7 surface there are two series of peaks which are not in the spectra of the unreconstructed (111)1×1 surface. These peaks are interpreted by a two-step model; electrons are excited into surface-state resonances lying above the vacuum level, from which states they emerge into the vacuum. The dispersion curves of these states are presented and discussed.

Measurements of the energy and angular dependence of secondary-electron emission (EADSEE) are made to gain a more detailed understanding of all the processes involved in the emission. Previous measurements have yielded data that fall into two classes: structureless spectra whose intensity at any one energy varies as the cosine of the angle between the direction of emergence and the surface normal[1]; or structure other than this, which has been related to features in the density of bulk electronic states.[2] Here I report a high-resolution study of EADSEE from a single-crystal Si(111)7×7 surface.

The apparatus consists of an electron monochromator source, fixed within the chamber, a sample holder that can be manipulated to bring the crystal to any orientation with respect to the incident beam, and an electron spectrometer which can rotate about the crystal, thus varying the take-off angle of the electrons being analyzed. The surface traced out by the entrance axis of the spectrometer is coplanar with the incident beam. This equipment is housed in a stainless-steel chamber, with a pressure of less than 2.5×10^{-11} Torr, a magnetic field less than 2 mG, and a low, but unknown, electric field. For the data presented the angular resolution is about 1.25°, and the energy resolution 0.1 eV.[3]

The silicon crystal used was cut from a 4-Ω-cm n-type wafer. This sample was chemically cleaned in the manner described by Chang,[4] mounted in tantalum slips, and cleaned in the vacuum by heating to 870°C for about an hour.[4] The surface thus prepared gave a distinct (111)-7×7 elastic-low-energy-electron-diffraction (ELEED) pattern, as measured by angular scans of the elastic peak in the $[2\bar{1}\bar{1}]$ and $[11\bar{2}]$ azimuths.

For fixed incident-beam conditions the energy spectrum was measured at each of a series of angles of emergence. The zero of kinetic energy was determined from the threshold of the spectrum of electrons emerging along the surface normal, in the usual manner.[1,2]